

Production of hypernuclei in peripheral relativistic ion collisions.

A.S. Botvina^{1,2}, K.K. Gudima³, J. Pochodzalla^{2,4}

¹*Institute for Nuclear Research, Russian Academy of Sciences, 117312 Moscow, Russia*

²*Helmholtz-Institut Mainz, J.Gutenberg-Universität, 55099 Mainz, Germany*

³*Institute of Applied Physics, Academy of Sciences
of Moldova, MD-2028 Kishinev, Moldova and*

⁴*Institut für Kernphysik and PRISMA Cluster of Excellence,
J.Gutenberg-Universität Mainz, D-55099 Germany*

(Dated: August 24, 2018)

Abstract

Within a dynamical and statistical approach we study the main regularities in production of hypernuclei coming from projectile and target residues in relativistic ion collisions. We demonstrate that yields of hypernuclei increase considerably above the energy threshold for Λ hyperons, and there is a saturation for yields of single hypernuclei with increasing the beam energy up to few TeV. Production of specific hypernuclei depend very much on the isotopic composition of the projectile, and this gives a chance to obtain exotic hypernuclei that may be difficult to reach in traditional hypernuclear experiments. Possibilities for the detection of such hypernuclei with planned and available relativistic ion facilities are discussed.

PACS numbers: 21.80.+a, 25.70.Mn, 25.70.Pq, 25.75.-q

I. INTRODUCTION

Nuclear reactions induced by energetic ions lead to abundant production of strange baryons (hyperons). When hyperons are captured by nuclei, hypernuclei are formed whose lifetime are significantly longer than the typical reaction times. These hypernuclei are an important tool to study the hyperon–nucleon (YN) and hyperon–hyperon (YY) interactions at low energies ($Y = \Lambda, \Sigma, \Xi, \Omega$), in order to overcome the limited experimental possibilities existing in elementary scattering experiments. Double- and multi-strange nuclei are especially interesting, because they can provide information about the hyperon–hyperon interaction and hyper-matter properties at low temperature. Furthermore, hypernuclei can help to investigate the structure of conventional nuclei too [1, 2], and extend the nuclear chart into the strangeness sector [3–5]. It is also known that hyper-matter should be produced at high nuclear densities, which are realized in the core of neutron stars [6]. Therefore, production of hypernuclei (particular those with extreme isospin) in the laboratory is important for many fields of research.

Typical observables for hypernuclei are ground-state masses, energy levels, and decay properties [2]. The theoretical studies are mainly concentrated on calculating the structure of nearly cold hypernuclei with baryon density around the nuclear saturation density, $\rho_0 \approx 0.15 \text{ fm}^{-3}$. However, a quite limited set of reactions was generally used for producing hypernuclei: Reactions with the production of few particles, including kaons, are quite effective for triggering single hypernuclei, and by using kaon beams one can produce double hypernuclei. The goal of this paper is to demonstrate that one can essentially extend the frame of hypernuclear studies and produce exotic hypernuclei if new many-nucleon reactions are involved.

We should remember that hyperons were discovered in the 1950-s in reactions of nuclear multifragmentation induced by cosmic rays [7]. During the last 20 years of research a great progress was made in investigation of the multifragmentation reactions, mainly associated with heavy-ion collisions (see, e.g., [8–11] and references therein). This gives us an opportunity to apply a well known theoretical method adopted for description of these reactions for production of hypernuclei too [12, 13]. On the other hand, it was noticed long ago that the absorption of hyperons in spectator regions after peripheral nuclear collisions is an effective way for producing hypernuclei [14–17]. Corresponding experimental evidences have been

reported [18, 19]. Also central collisions of relativistic heavy ions can lead to productions of light hypernuclei [20]. Recent sophisticated experiments have confirmed observations of hypernuclei in such reactions, in both peripheral [21] and central collisions [22].

We want to pay special attention to formation of hypernuclei in spectator region of peripheral relativistic ion collisions. Current research concerns light hypernuclei produced in reactions with light projectiles [21], which were previously obtained in other reactions. There is also a promising opportunity to study production of large and exotic hypernuclei coming from reactions with large projectiles and targets [17, 23]. In particular, multifragmentation decay of excited hyper-spectator matter [3, 12, 13], and the Fermi-break-up of excited light hyper-spectators [24, 25] are perspective mechanisms. Below we undertake a systematic investigation of how new and exotic hypernuclei can be obtained in future experiments. For this purpose we use a hybrid dynamical and statistical approach, which is widely accepted as one of the best tool for description of fragmentation and multifragmentation reactions.

II. FORMATION OF HYPER-RESIDUES

A mechanism of peripheral relativistic heavy-ion collisions has been established in many experimental and theoretical studies. In the simplified picture nucleons from overlapping parts of the projectile and target (participant zone) interact strongly with themselves and with other hadrons produced in primary and secondary collisions. Nucleons from non-overlapping parts do not interact intensively, and they form residual nuclear systems, which we call spectator residues or spectators. In all transport models the production of hyperons is associated with nucleon-nucleon collisions, e.g., $p+n \rightarrow n+\Lambda+K^+$, or collisions of secondary mesons with nucleons, e.g., $\pi^++n \rightarrow \Lambda+K^+$. Strange particles may be produced in the participant zone, however, particles can re-scatter and undergo secondary interactions. As a result the produced hyperons populate the whole momentum space around the colliding nuclei, including the vicinity of nuclear spectators. Such hyperons can be absorbed by the spectators if their kinetic energy (in the rest frame of the spectator) is lower than the potential generated by neighbouring spectator nucleons. The process of formation of spectator hyper-matter was investigate in Ref. [17] within the transport approaches, Dubna cascade model (DCM) [26, 27], and Ultra-relativistic Quantum Molecular Dynamics (UrQMD) model [28, 29]. It was concluded that already at beam energy of 2 A GeV hyper-spectators

with one absorbed Λ can be noticeably produced. While at energy of few tens of GeV per nucleons formation of double- and multi-strange hyper-spectators become feasible.

Here we use the DCM transport approach, therefore, it should be recalled in more details. The DCM is based on the Monte-Carlo solution of a set of the Boltzmann-Uehling-Uhlenbeck relativistic kinetic equations with the collision terms, including cascade-cascade interactions. For particle energies below 1 GeV it is effective to consider only nucleons, pions and deltas. The model includes a proper description of pion and baryon dynamics for particle production and absorption processes. In the original version the nuclear potential is treated dynamically, i.e., for the initial state it is determined using the Thomas-Fermi approximation, but later on its depth is changed according to the number of knocked-out nucleons. This allows one to account for nuclear binding. The Pauli principle is implemented by introducing a Fermi distribution of nucleon momenta as well as a Pauli blocking factors for scattered nucleons. At energies higher than about 10 GeV, the Quark-Gluon String Model (QGSM) is used to describe elementary hadron collisions [27, 30]. This model is based on the $1/N_c$ expansion of the amplitude for binary processes where N_c is the number of quark colours. Different terms of the $1/N_c$ expansion correspond to different diagrams which are classified according to their topological properties. Every diagram defines how many strings are created in a hadronic collision and which quark-antiquark or quark-diquark pairs form these strings. The relative contributions of different diagrams can be estimated within Regge theory, and all QGSM parameters for hadron-hadron collisions were fixed from the analysis of experimental data. The break-up of strings via creation of quark-antiquark and diquark-antidiquark pairs is described by the Field-Feynman method using phenomenological functions for the fragmentation of quarks, antiquarks and diquarks into hadrons. The modified non-Markovian relativistic kinetic equation, having a structure close to the Boltzmann-Uehling-Uhlenbeck kinetic equation, but accounting for the finite formation time of newly created hadrons, is used for simulations of relativistic nuclear collisions. One should note that QGSM considers the two lowest $SU(3)$ multiplets in mesonic, baryonic and antibaryonic sectors, so interactions between almost 70 hadron species are treated on the same footing. The above noted two energy extremes were bridged by the QGSM extension downward in the beam energy [31].

Within this model the absorption of Λ hyperons by spectators is described in Ref. [17]. It takes place if a hyperon kinetic energy in the rest frame of the residual spectator is lower

than the attractive potential energy, i.e., the hyperon potential. This potential is calculated by taking into account the local density of the spectator residues, which can be less than the normal nucleus density. In the calculations we follow the propagation of all particles including Λ -hyperons during the whole reaction time, up to about 100 fm/c, and take into consideration secondary rescattering/interaction processes, which may lead to the hyperon production, the hyperon absorption, and making free the absorbed hyperons.

The DCM was already successfully proved extensively in different kind of reactions for description of experimental data including particle production [26], fragmentation of spectators [32], and production of Λ hyperons [17]. Since in this work we show results for very high energy also, it is instructive to demonstrate how this model describe general yields of light particles, which can cause for secondary reactions leading to strangeness production in the spectator kinematic region. In Fig. 1 we show comparisons of DCM calculations (with the QGSM elementary interaction acts) with experimental data on rapidity distribution of pions obtained in proton interactions at $\sqrt{s}=17.2$ GeV [33] and at $\sqrt{s}=200$ GeV [34]. One can see that the model is quite good in the reproduction of pion rapidities. It is important that they can go far beyond the projectile and target rapidities, which are $y_{cm} \approx_{-}^{+}2.9$ and $y_{cm} \approx_{-}^{+}5.4$ for these cases, respectively. Such comparisons give us some confidence that the model can be used for description of subsequent processes initiated by these particles, which also include hyperon production in reactions with spectator nucleons. Then, similar as we have found at lower energies [17], these hyperon can be captured by nuclear residues.

III. DEPENDENCE OF YIELDS OF HYPER-SPECTATOR RESIDUES ON INCIDENT ENERGY

In the following we investigate how the absorption of Λ hyperons by spectator residues evolves with incident projectile energy. As mentioned above, in the DCM calculations we use a prescription for the hyperon absorption elaborated in Ref. [17], which gives results similar to ones obtained in other transport (UrQMD) calculations. For clarity, we consider collisions of symmetric ions, both light and heavy ones.

In Fig. 2 we demonstrate evolution of yields of hyper-residues in the very broad range of the projectile incident energies (in laboratory system) for carbon, nickel and lead collisions. The DCM calculations were done taking into account all impact parameters as in experiment.

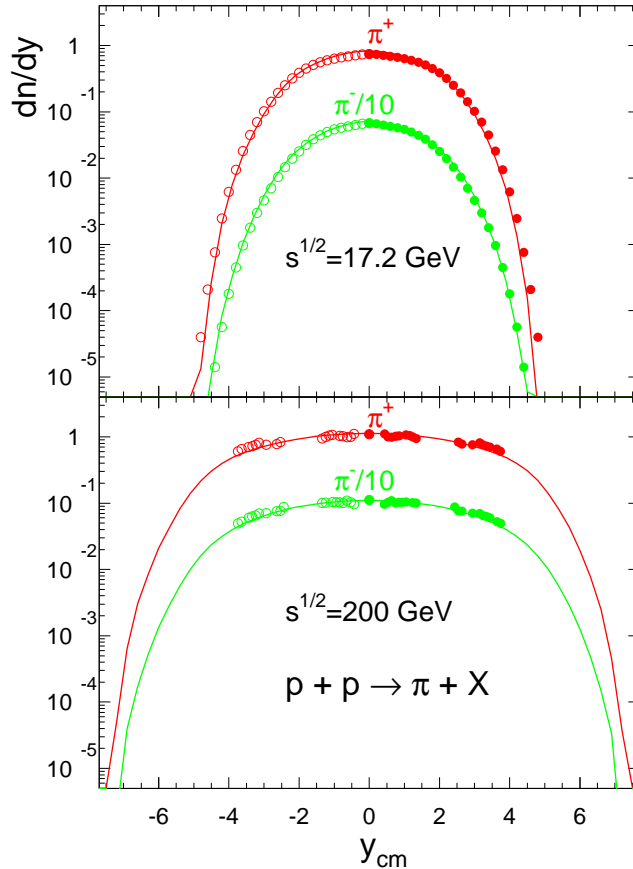


FIG. 1: (Color online) Distribution of π^+ and π^- yields versus the center-of-mass rapidity y_{cm} in proton-proton collisions at energies of $s^{1/2}=17.2 \text{ GeV}$ (top panel) and $s^{1/2}=200 \text{ GeV}$ (bottom panel). Solid points are experimental data [33, 34] (open ones - their symmetric reflections in the rapidity axis), solid lines are DCM calculations.

For example, in this case in carbon reactions more than 90% events contain the spectator residues with the mass number $A > 1$. We note that usually one hyperon is absorbed in these reactions. The absorption of two and more hyperons is also possible, especially for heavy nuclei. However, probability of the second absorption is considerably lower [17] and it does not influence the general behaviour of the curves. One can see a rapid increase of the yields with energy at low incident energies, which is related to the threshold character of Λ production. The yield per inelastic event is much larger for the case of heavy projectile. This has a simple explanation: in collisions of many nucleons the strange particles can be more

abundantly produced and more absorption events can take place at large residual nuclei. At energies around 10 GeV per nucleon we observe a nearly saturation behaviour. This means that we do not need too high energies to produce single hypernuclei. However, we should be careful at this point: The production of double and multiple hypernuclei can increase with the incident energy [17]. This effect will be investigated in next works.

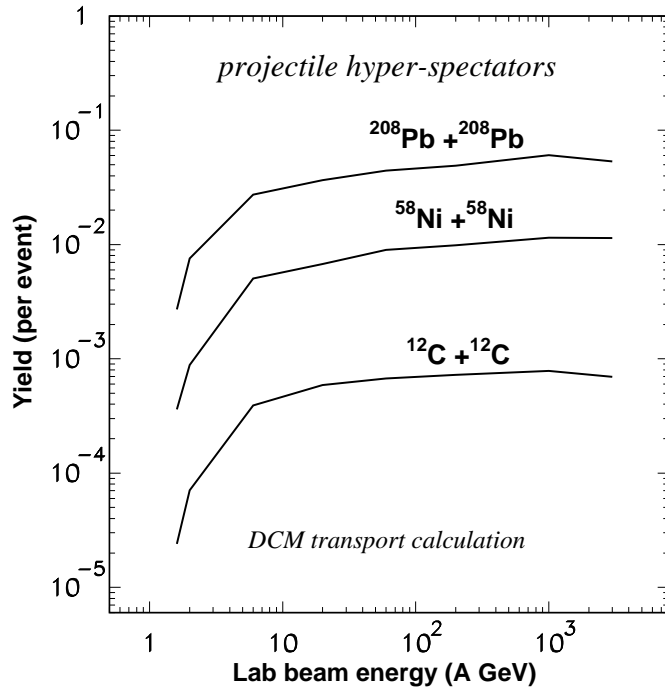


FIG. 2: Yields of hyper-residues of projectiles in collisions of ^{12}C , ^{58}Ni , and ^{208}Pb beams with the same targets, as function of the incident energy. The DCM calculations are integrated over all impact parameters, and normalized to one inelastic collision event.

As was shown previously [17] these hypernuclei residues have a broad mass distribution. Their masses are defined after all fast nucleons leave the residues and low-energy nucleons are captured inside them. The examples of such distributions at moderate beam energies are shown in Ref. [17] (for large nuclei) and in Ref. [24] (for small nuclei). However, as one can see from Fig. 3 the average masses of these residues do not change practically over all projectile energies under investigation.

It is very instructive to analyze the rapidity distribution of produced hyper-residues and compare it with the distribution of free Λ hyperons. It is shown in Fig. 4 that such distributions for produced Λ s are quite wide, and evolve from a Gaussian-like one in central

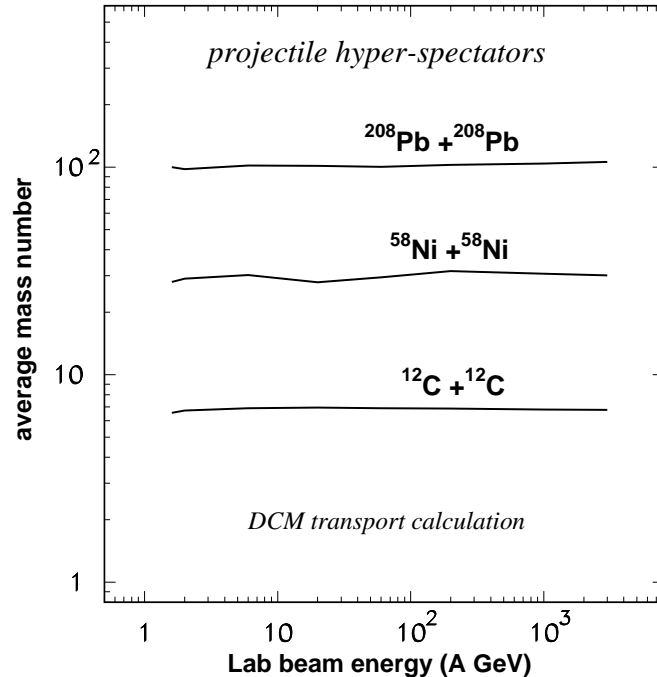


FIG. 3: Average mass number of the projectile hyper-residues, shown in Fig. 2, as function of the incident energy.

midrapidity zone at low beam energies to plateau-like and double-peak ones at high energy. This tells us that the main source of Λ s is not direct nucleon-nucleon collisions in the participant (overlapping) zone, but it is related to secondary hadron interactions. This point was already discussed in details in Ref. [17], where the space-time evolution of the absorption at 20 A GeV was demonstrated, and it was shown that the DCM describes the rapidity distribution of Λ well at ~ 2 GeV per nucleon. Unfortunately, there are no experimental data for large rapidity at high energy. However, as we see from Fig. 1 the model is able to describe elementary experimental data for pion production for all rapidities at $\sqrt{s}=17.2$ corresponding to the beam energy of 158 A GeV. Those distributions go far beyond the projectile and target rapidities, and interactions of these mesons with residues contribute to the hyperon production too.

It is natural that the existence of large nuclear residues favors both production and capture of hyperons in secondary reactions. As seen from Fig. 4, for rapidities higher than the projectile (and target) ones the yield of free Λ drops essentially. It is partly related with absorption of hyperons by spectator residues. On the other hand decreasing the number of

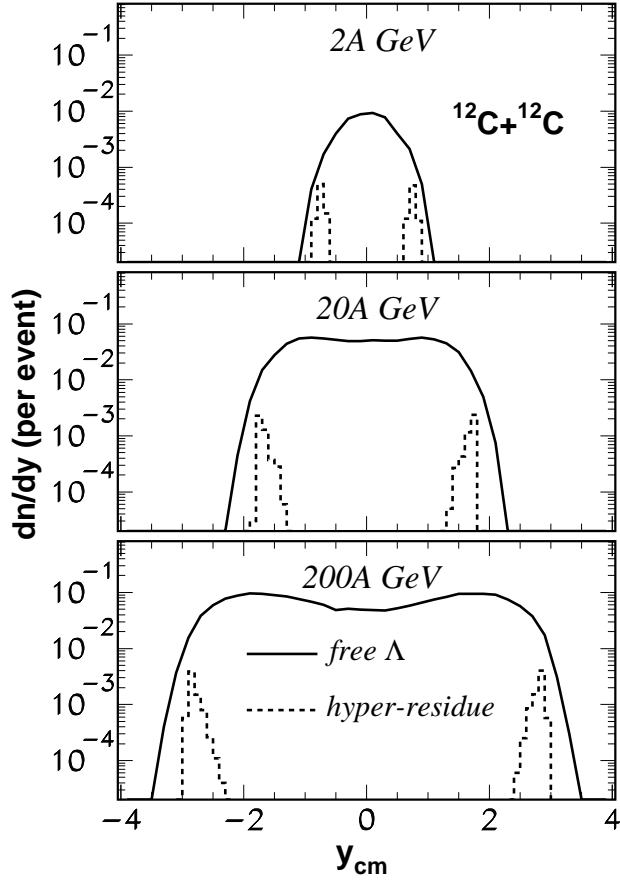


FIG. 4: Rapidity distributions in the system of center-of-mass y_{cm} of free Λ (solid curves) and projectile and target hyper-residues (dashed histograms) normalized per one inelastic event in $^{12}\text{C}+^{12}\text{C}$ interactions. Top, middle, and bottom panels are for collisions with 2, 20 , and 200 GeV per nucleon energy, respectively, as calculated with the DCM.

baryons and secondary particles (like pions, see Fig. 1) does not give a chance to produce many new Λ hyperons in the region above the spectator rapidity.

The results shown in Figs. 2 , 3 and 4 tell us that the hyperon capture happens as a result of an universal stochastic process. As was discussed previously [12, 15, 17, 24] the production of low-energy Λ which can be potentially captured is related to many rescatterings and secondary interactions involving produced particles. The yield of these hyperons is mainly determined by the amount of secondary particles in the vicinity of the projectile rapidity. However, when the energy exceeds the threshold essentially ($\gtrsim 10 A$ GeV) the hyperons

and other produced light particles tend to populate the rapidity space broadly at all beam energies: For example, one can see from Fig. 4 that around the residue rapidity the ratio of 'background' free Λ s to the hyper-residues remains nearly the same, a little bit less than factor 10. On the other hand the residues can loose certain number of nucleons during the particle interaction process. Depending on this interaction the number of hyperons can fluctuate event by event too. Nevertheless, there is a balance between the amount of hyperons with energies suitable for capture and the number of residual nucleons on which this capture may happen. This can explain that the mean mass number of hyper-residues is practically the same for all energies (Fig. 3). The predicted saturation of the production at high energies (Fig. 2) indicate that there are opportunities to study projectile- and target-like hypernuclei at different relativistic heavy-ion facilities (e.g., GSI/FAIR, JINR/NICA, RHIC, LHC) with comparable yields.

One should remember, however, that these hyper-residues are excited. During the next stage of the reaction they disintegrate in normal nuclei and nuclei containing hyperons. This process can be described within the models of multifragmentation [3, 12] and the Fermi-break-up [24, 25]. The processes of fission and evaporation of hot hypernuclei can also take place by analogy with behaviour of normal excited nuclei. Presently, the experimental methods for identification of light hypernuclei are most reliable [2, 21]. For this reason and to guide future experimental studies we concentrate in the next sections on predictions for light ion reactions.

IV. PRODUCTION OF LIGHT HYPERNUCLEI

The general information on the formation of light projectile hyper-residues and its evolution with beam energy is displayed in Figs. 2–4 for the case of carbon-carbon collisions. As was mentioned, their de-excitation caused by strong interaction can be described by the Fermi-break-up model [25]. The procedure of our analysis was the following: For all inelastic $^{12}\text{C} + ^{12}\text{C}$ collisions we had found mass number, charge, strangeness, excitation energy and kinematic characteristics of the projectile residues within the DCM. The Fermi-break-up model (FBM) was used afterwards to describe their disintegration. We use the connection of dynamical and statistical models with parameters which have provided the best reproduction of experimental data analyzed in Ref. [24]. As was there demonstrated, reasonable variation

of excitation energies of hyper-residues would lead to slightly different results. However, the results for the yields will not change by more than 30%, which is typical precision for the hybrid calculations. This is also a characteristic accuracy in description of experimental data within an approach including dynamical transport plus statistical decay for normal fragment production in such collisions of nuclei. It is sufficient for our present purposes intended to give a qualitative understanding of the processes for future experimental needs.

It is necessary to mention that production of light clusters is sometimes related to coalescence of individual nucleons. However, this mechanism describes experimental data usually in midrapidity region, where there are many free particles [20, 26]. It looks like that this mechanism is responsible for production of lightest hypernuclei and anti-hypernuclei at relativistic central collisions at RHIC and LHC [22, 35]. In the region of spectator residues the coalescence may not be effective for description of the data [24], and systematic comparison with experiment is needed.

In Fig. 5 we show results of our hybrid DCM plus FBM calculations for carbon-carbon collisions in the projectile energy range from the threshold of Λ production to 3 TeV per nucleon. The highest energy corresponds to LHC ion beams: In this respect we cover energies available with modern accelerators. We considered production of both well known hypernuclei (as ${}^4_{\Lambda}\text{H}$, ${}^3_{\Lambda}\text{H}$, ${}^7_{\Lambda}\text{Be}$) and recently discovered an exotic neutron-rich ${}^6_{\Lambda}\text{H}$ [36]. Formation of a hypothetical Λ -neutron bound state ($\text{N}\Lambda$) was discussed previously in Refs. [24, 35, 37], therefore, we show predictions for $\text{N}\Lambda$ systems too. One can see that evolution of the hypernuclei's yield with energy demonstrates the same feature as the production of the hypernuclear residues (Fig. 2). Namely, there is a rapid increase around the threshold and a saturation-like behaviour at higher energies. It is quite obviously, since production of particular hypernuclei is regulated by statistical decay of excited residues, which properties do not change noticeably with the beam energy (see, e.g., masses in Fig. 3). We see that smaller hypernuclei have usually higher probability, mainly, because the excited hyper-residues are initially rather small (in average) and they disintegrate into small nuclei. The phase space favors also disintegration of such residues into small pieces, since there is no considerable energy gain coming from the hyperon binding in the case of formation of nuclei with larger mass numbers.

It is important to analyze how the yield of particular hypernuclei depends on mass number and charge of colliding nuclei. This problem was already addressed in Ref. [3] in relation

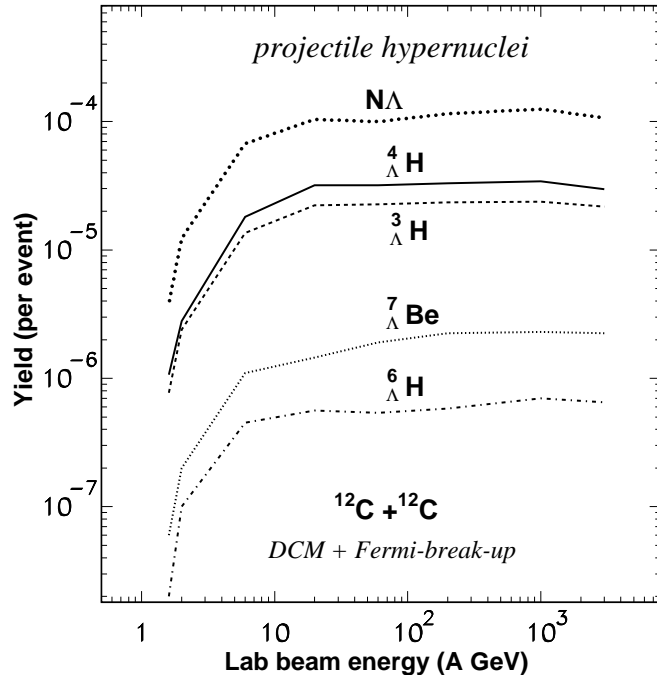


FIG. 5: Yields of particular hyper-nuclei (see figure and the text) obtained from projectile residues in collisions of ^{12}C with ^{12}C versus projectile energy in laboratory system. The hybrid DCM and FBM calculations are integrated over all impact parameters, and normalized to one inelastic collision event.

to production of hypernuclei beyond neutron and proton drip-lines. In our case we have performed DCM and FBM calculations by taking different isotopes of carbon as projectiles. The beam energy of 20 A GeV was adopted because it is expected for FAIR facility at GSI. The considered beams could be easily obtained there with the FRagment Separator (FRS) [38, 39]. Figure 6 demonstrates that yields of specific projectile hypernuclei are very sensitive to isotope composition of the projectile. One can considerably increase production of neutron-rich hypernuclei when we take neutron-rich beams (e.g., ^{16}C). For example, the yield of exotic ${}^6_{\Lambda}\text{H}$, may increase by two orders, and this makes its observation much easier. If we take proton-rich beams (e.g., ^{10}C), production of proton-rich hypernuclei, like ${}^7_{\Lambda}\text{Be}$, becomes more prominent. We believe, in reactions initiated by different isotopes one can obtain all kinds of hypernuclei which may exist. In addition, by looking at relative yields of hypernuclei we can better investigate the reaction mechanism and properties of hyper-matter at low temperature [12, 24].

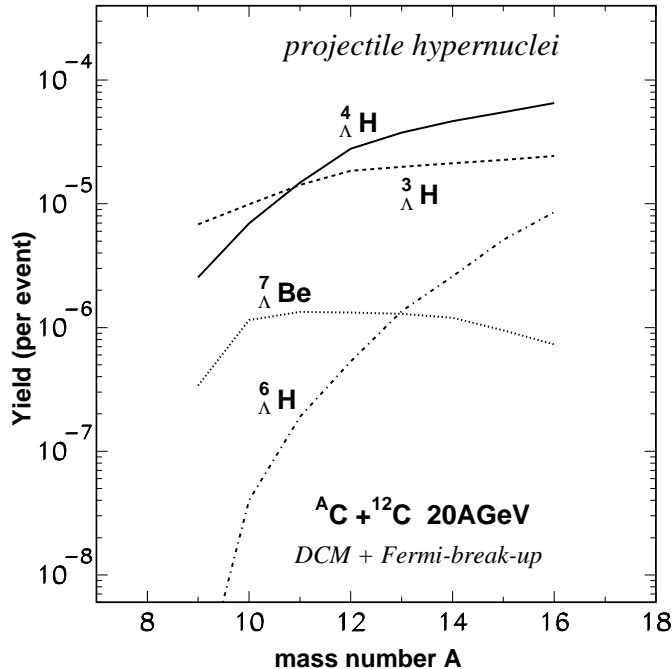


FIG. 6: The same as in Fig. 5, but in collisions of projectile carbon isotopes with target ${}^{12}\text{C}$ versus the isotope mass number A. The beam energy is 20 GeV per nucleon.

V. IDENTIFICATION OF HYPERNUCLEI

The suggested above reaction mechanisms are very promising for producing hypernuclei. In particular, one can use exotic neutron-rich and neutron-poor projectiles [3] which are not possible to use as targets in traditional hyper-nuclear experiments with meson and electron beams [1, 2], because of their short lifetime. In addition, one can study the equation of state and phase transition in hypermatter at low and moderate temperatures similar as it was done in normal nuclear matter [8–10, 40]. An essential advantage of peripheral relativistic collisions over central ones is that in the last ones only light hypernuclear species may be formed because of the high fireball temperature [20]. We avoid too high temperatures and we do not see any practical limitation on the production of large hypernuclei in peripheral collisions. Moreover, in such collisions we can accumulate strangeness in the projectile residues [17] and move step-by-step to multi-hyperon systems. However, an important question is if it is possible to identify hypernuclei reliably on the background of products of various nuclear interactions which take place in relativistic nucleus-nucleus collisions. We

feel rather optimistic in this respect because of previous successful observation of hypernuclei [21, 22, 35]. However, we believe it would be very useful for future experiments to show model calculations of the background and make its comparison with the expected signal.

Presently, the main channel for identification of light hypernuclei is their pionic decay. For example, a weak process ${}^3_{\Lambda}\text{H} \rightarrow \pi^- + {}^3\text{He}$, with a characteristic lifetimes around ~ 200 picoseconds can be seen in the experiments [21, 22, 35]. The background of this process consists of correlations of π^- and ${}^3\text{He}$ coming from other sources: The observed π^- are mainly obtained in strong interactions of various particles, and ${}^3\text{He}$ can be produced as a result of decay of non-strange excited spectator residues. In Fig. 7 we show general rapidity distribution of π^- and non-strange residues calculated with DCM for collisions of ${}^{12}\text{C}$ projectile with ${}^{12}\text{C}$ target at beam energies of 2, 20, and 200 GeV per nucleon. If compare it with a similar figure for hyperons and strange residues (Fig. 4) one can see that yields of non-strange particles are much larger. We see that pions overlap essentially the spectator residues, therefore, their correlation with fragments produced after disintegration of spectators must be investigated. On the other hand, we see also from Figs. 4 and 7 that for these processes with residues a simple 'participant-spectator' picture of reaction is not very precise. After nucleus-nucleus collision a residue fly in a dilute 'cloud' of particles, mostly, light pions. Secondary interactions between such particles and the residue are important for the residue's strangeness content.

The corresponding DCM and FBM calculations of correlations of pions and fragments were performed and the results are demonstrated in Fig. 8: We analyze invariant masses of π^- and deuterons, and π^- and ${}^3\text{He}$. The first pair is interesting as decay products of a possible hypothetical Λ -neutron (NA) bound system [35, 37]. The second pair is typical for ${}^3_{\Lambda}\text{H}$ weak decay. In modern experimental analyses a precision for determination of invariant masses is around 5–10 MeV [21, 22, 35]. For this reason we have also adopted 10 MeV invariant mass intervals and counted event by event how many pairs fall to these intervals in the events where the both particles are produced. Afterwards, total normalization to the number of inelastic events was performed. The most interesting part of the distributions is a rise around the two particle threshold and its following transformation to a plateau-like behaviour caused by a very broad rapidity range of produced pions. Within ~ 50 MeV above the threshold we expect a signal of the hypernucleus decay.

It is important that the signal should be clearly seen above the background. By examining

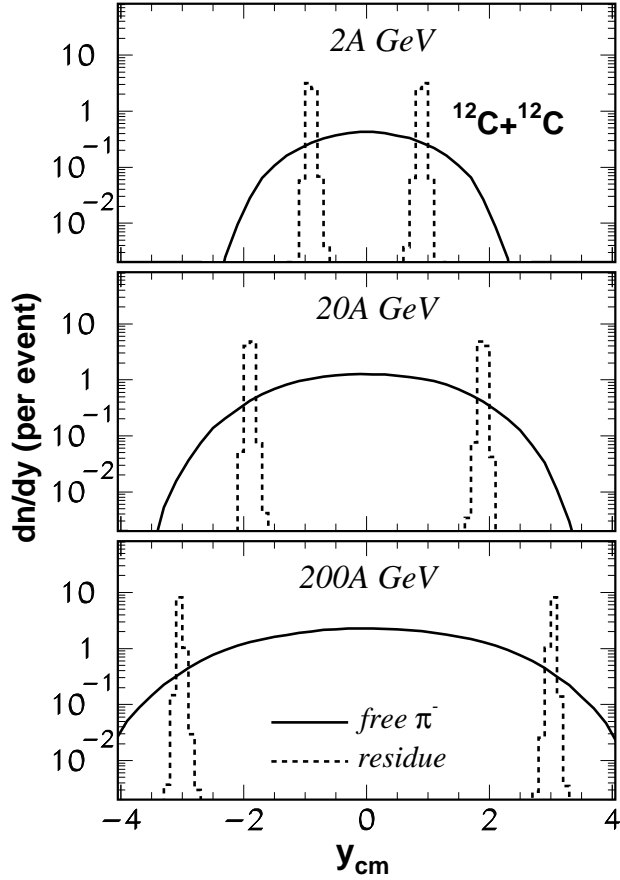


FIG. 7: Rapidity distributions in the system of center-of-mass \mathbf{y}_{cm} of free π^- (solid curves) and projectile and target spectator residues (dashed histograms) normalized per one inelastic event in $^{12}\text{C}+^{12}\text{C}$ interactions. Top, middle, and bottom panels are for collisions with 2, 20 , and 200 GeV per nucleon energy, respectively, as calculated with the DCM.

$^3_{\Lambda}\text{H}$ hyper-nucleus we can estimate from Fig. 5 its probability as about $2.5 \cdot 10^{-5}$ per event at 20A GeV. Whereas the background pairs in the 10 MeV interval around this hypernucleus mass reach $\sim 5 \cdot 10^{-3}$ per event (Fig. 8). Improving energy resolution will make the signal separation better. However, the ratio of signal to background is expected to be around 1% for this nucleus. This ratio may increase to few percent for the NA states. In these cases experimenters must take into account the time delay of the pionic decay and filter the corresponding events. The relatively long lifetime of hypernuclei allows to select a displaced vertex of correlated particles and to decrease the background significantly. For example, in

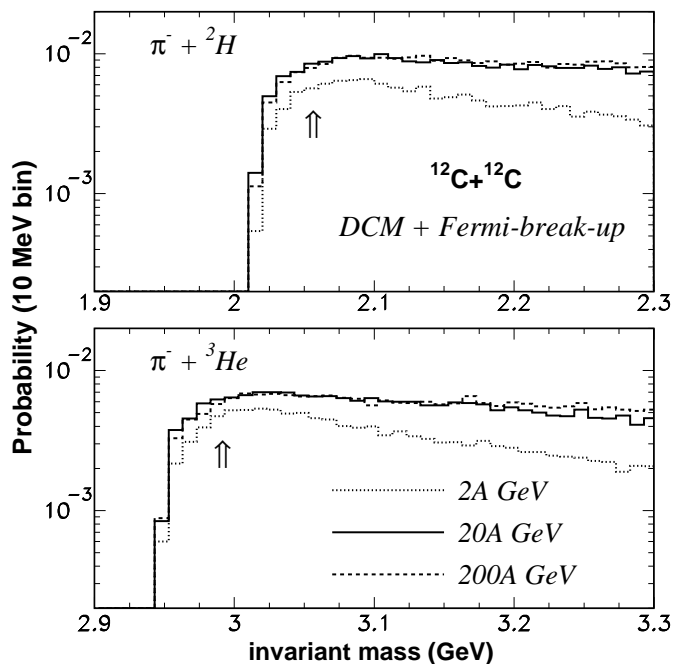


FIG. 8: Invariant mass distributions of the π^- plus ${}^2\text{H}$ pairs (top panel), and the π^- plus ${}^3\text{He}$ pairs (bottom panel) obtained in carbon–carbon collisions at energies of 2 GeV per nucleon (dotted histograms), 20 GeV per nucleon (solid histograms), and 200 GeV per nucleon (dashed histograms). The event by event calculations are performed within the DCM and Fermi-break-up models. The count number of the pairs in 10 MeV bins of invariant mass are normalized per inelastic event and noted as probability. Arrows mark the invariant masses corresponding to an NA bound state [37] and to ${}^3_{\Lambda}\text{H}$ nuclei.

central collision experiments, where many hundreds background pions are produced, it was possible to increase the ratio of signal to background up to 20–30% in such a way [22, 35].

The situation with identification of projectile hypernuclei may be better because of large γ -factors increasing their lifetime. In recent HypHI experiments [21] at relatively low energies (2A GeV) the signal and lifetime of projectile hypernuclei were reliably measured even at low statistics. These hypernuclei can propagate at beam energies of 2A GeV, 20A GeV, 200A GeV and 3A TeV about 20 cm, 130 cm, 13 meters, and nearly 200 meters, respectively, before their weak decay. Such a space separation from the place where they were produced increases chances on their identification, since many particles contributing to the background

shown in Figs. 8 can be filtered out.

Actually, the experimental set up for this measurement should be constructed by taking into account the accelerator energy. It is interesting that some already existing detectors might be suitable for this measurement. For example, at the distance around 120 meters from the ALICE detector at LHC a Zero Degree Calorimeter (ZDC) is located [41]. Originally ZDC was designed to measure neutrons and one-charged particles coming from decay of spectator residues for better selection of central events. However, it is the exact place where neutral and one-charged projectile hypernuclei (like exotic Λ system and ${}^6_{\Lambda}\text{H}$) will decay. Many other free hyperons flying with similar rapidities will reach ZDC too. A fixed target providing much higher luminosity in comparison with colliding beams would be sufficient for this experiment.

VI. CONCLUSION

We investigate new promising reactions for production of hypernuclei in peripheral relativistic ion collisions over a wide energy range. Hadron interactions during dynamical stage of the process can lead to production of hyperons, which are captured by spectator residues. Disintegration of these hot residues leads to production of hypernuclei. This kind of reactions is well known in nuclear physics and it is associated with fragmentation and multifragmentation of relativistic residual nuclei. It is described quite reliably by hybrid (dynamical and statistical) models. Presently, production of projectile residues is widely used for synthesizing new elements, producing nuclei around the proton and neutron drip-lines, investigating the phase transition in nuclear matter at subnuclear densities. Including hyperons interacting in nuclear matter analogous to nucleons will open new opportunities for this study and can extend it in the direction of strangeness sector towards multi-strange nuclear systems at low temperatures. In addition, this method for obtaining hypernuclei has some advantages over the currently used ones: One can use exotic unstable projectiles and, as a result, to produce exotic hypernuclei, which may not be reachable in other ways.

The model calculations performed in this paper indicate that this production mechanism is effective already at beam energies $\gtrsim 2$ GeV per nucleon. At the energies more than 10 GeV per nucleon a saturation of the yields of single hypernuclei takes place. For this reason these reactions can be investigated at future FAIR at GSI and NICA at JINR facilities, as well as

at presently operating RHIC and LHC facilities. Depending on the size of colliding nuclei the cross-section for formation of excited hyper-residues in the saturation region is about $\sim 1-10^2$ millibarn. We show also probabilities for production of specific light hypernuclei and evaluate the background conditions for their measurement. By selecting neutron-rich and neutron-poor isotope beams it is possible to increase yields of exotic hypernuclei by more than one order of magnitude. We are convinced that hypernuclear and nuclear physics will benefit strongly from exploring new ways for production of hypernuclei associated with fragmentation of spectator residues.

Acknowledgments

We thank M. Bleicher, I. Mishustin, and T. Saito for discussions. This work was supported by the Helmholtz-Institut Mainz. A.S.B. thanks the Frankfurt Institute for Advanced Studies J.W. Goethe University and the Institut für Kernphysik of J.Gutenberg-Universität Mainz for hospitality. We also acknowledge the support by the Research Infrastructure Integrating Activity Study of Strongly Interacting Matter HadronPhysics3 under the 7th Framework Programme of EU (SPHERE network).

-
- [1] H. Bando, T. Mottle, and J. Zofka, *Int. J. Mod. Phys.* **A5**, 4021 (1990).
 - [2] O. Hashimoto, H. Tamura, *Prog. Part. Nucl. Phys.* **57**, 564 (2006).
 - [3] N. Buyukcizmeci, A.S. Botvina, J. Pochodzalla, and M. Bleicher, arXiv:1307.3652v1, 2013; accepted in *Phys. Rev. C*.
 - [4] J. Schaffner, C.B. Dover, A. Gal, C. Greiner, and H. Stoecker, *Phys. Rev. Lett.* **71**, 1328 (1993).
 - [5] W. Greiner, *J. Mod. Phys.* **E5**, 1 (1995).
 - [6] J. Schaffner-Bielich, *Nucl. Phys. A* **804**, 309 (2008).
 - [7] M. Danysz and J. Pniewski, *Philos. Mag.* **44**, 348 (1953).
 - [8] J.P. Bondorf, A.S. Botvina, A.S. Iljinov, I.N. Mishustin, and K. Sneppen, *Phys. Rep.* **257**, 133 (1995).
 - [9] H. Xi *et al.*, *Z. Phys. A* **359**, 397 (1997).

- [10] R.P. Scharenberg *et al.*, Phys. Rev. C **64**, 054602 (2001).
- [11] R. Ogul *et al.*, Phys. Rev. C **83**, 024608 (2011).
- [12] A.S. Botvina and J. Pochodzalla, Phys. Rev. C **76**, 024909 (2007).
- [13] S.Das Gupta, Nucl. Phys. A **822**, 41 (2009); V.Topor Pop, S.Das Gupta, Phys. Rev. C **81**, 054911 (2010).
- [14] M. Wakai, H. Bando and M. Sano, Phys. Rev. C **38**, 748 (1988).
- [15] Z.Rudy, W.Cassing *et al.*, Z. Phys. A **351**, 217 (1995).
- [16] Th. Gaitanos, H. Lenske, and U. Mosel, Phys. Lett. B **675**, 297 (2009).
- [17] A.S. Botvina, K.K. Gudima, J. Steinheimer, M. Bleicher, I.N. Mishustin, Phys. Rev. C **84**, 064904 (2011).
- [18] K.J. Nield *et al.*, Phys. Rev. C **13**, 1263 (1976).
- [19] S. Avramenko *et al.*, JETP Lett. **48**, 516 (1988); S. Avramenko *et al.*, Nucl. Phys. A **547**, 95c (1992).
- [20] J. Steinheimer, K. Gudima, A. Botvina, I. Mishustin, M. Bleicher, H. Stoecker. Phys. Lett. B **714**, 85 (2012).
- [21] T.R. Saito *et al.* (HypHI collaboration), Nucl. Phys. A **881**, 218 (2012). C. Rappold *et al.*, Nucl. Phys. A **913**, 170 (2013); arXiv:1305.4871, 2013.
- [22] The STAR collaboration, Science **328**, 58 (2010).
- [23] A.S. Botvina *et al.*, Nucl. Phys. A **881**, 228 (2012).
- [24] A.S. Botvina, I.N. Mishustin, J. Pochodzalla, Phys. Rev. C **86**, 011601 (R) (2012).
- [25] A.S. Lorente, A.S. Botvina, and J. Pochodzalla, Phys. Lett. B **697**, 222 (2011).
- [26] V.D. Toneev, K.K. Gudima, Nucl. Phys. A **400**, 173c (1983).
- [27] V.D. Toneev, N.S. Amelin, K.K. Gudima, S.Yu. Sivoklokov, Nucl. Phys. A **519**, 463c (1990).
- [28] M. Bleicher *et al.*, J. Phys. G **25**, 1859 (1999).
- [29] S. A. Bass *et al.*, Prog. Part. Nucl. Phys. **41**, 255 (1998).
- [30] N.S. Amelin, E.F. Staubo, L.S. Csernai *et al.*, Phys.Rev. C **44**, 1541 (1991).
- [31] N.S. Amelin, K.K. Gudima, S.Yu. Sivoklokov, V.D. Toneev, Sov. J. Nucl. Phys. **52**, 272 (1990).
- [32] A.S. Botvina, K.K. Gudima, A.S. Iljinov, and I.N. Mishustin, Phys. Atom. Nucl. **57**, 628 (1990).
- [33] C. Alt *et al.* (NA49 Collaboration), Eur. Phys. J. C**45**, 343 (2006).
- [34] “Brahms measurements in pp 62.4 and 200 GeV”, <http://theory.fnal.gov/trtles/Brahms-pp.pdf>

- [35] B. Dönigus *et al.* (ALICE collaboration), Nucl. Phys. A **904-905**, 547c (2013).
- [36] M. Agnello *et al.*, Nucl. Phys. A **881**, 269 (2012).
- [37] T.R. Saito (for HypHI collaboration), talks at ECT workshop 'Strange Hadronic Matter', Trento, Italy, 2011, <http://www.ectstar.eu/> ; NUFRA2011 conference, Kemer, Turkey, 2011, <http://fias.uni-frankfurt.de/historical/nufra2011/>.
- [38] Th. Aumann, Progr. Part. Nucl. Phys. **59**, 3 (2007).
- [39] H. Geissel *et al.*, Nucl. Inst. Meth. Phys. Res. B **204**, 71 (2003).
- [40] J. Pochodzalla, Prog. Part. Nucl. Phys. **39**, 443 (1997).
- [41] N. De Marco *et al.* (ALICE collaboration), J. Phys. Conf. Ser. **160**, 012060 (2009).